Modeling of Environmental Torques of a Spin-Stabilized Spacecraft in a Near-Earth Orbit

N. W. TIDWELL*
Honeywell Inc., Minneapolis, Minn.

This paper is concerned with modeling disturbance torques experienced by spin-stabilized spacecraft in a near-Earth orbit. A computer program developed to simulate the particular mission was used to evaluate the behavior of the torques, and a simulation was performed to determine the attitude effect of each torque relative to the untorqued vehicle. The magnetic interaction torques were the most significant in terms of spin decay. Torques caused by solar pressure and gravity gradient were the next most significant, while the aerodynamic torque was the least significant. The solar pressure and gravity gradient torques had the greatest effect on precession ($\Delta\phi$ and $\Delta\psi$). State prediction within 15.4-arc sec was possible for 5 min using only the residual magnetic moment and the eddy current torques in the vehicle model.

Nomenclature

A,C = inertia ratios
a_o,b_o,c_o = components of τ_B
$\mathbf{B}$ = Earth's magnetic field vector, gauss
C = a constant
c = speed of light in vacuum
cm = center of mass
d,h = width and length of solar panels, respectively
E_o = solar constant, 1396 w/m^2
$\hat{\mathbf{e}}_v$ = unit vector in direction of spacecraft orbital velocity
$\mathbf{H}$ = Earth's magnetic field strength = $\mathbf{B}/\mu_o$
$\bar{\bar{\mathbf{I}}}$ = moment of inertia dyadic of spacecraft
I_x,I_y,I_z = spacecraft principal moments of inertia
$\mathbf{J}$ = induced volume eddy current density
K = a coefficient based on the spacecraft dimensions and σ
K_1 = an integration parameter
L_2 = length from cm to solar panel end of spacecraft
$\mathbf{M}$ = residual magnetic moment vector
M_x,M_y,M_z = spacecraft body axes components of the residual magnetic moments
$\hat{\mathbf{n}}$ = unit outward normal to ds
P_e = radiation pressure
p_1,p_2,p_3 = coefficients based on spacecraft dimensions and σ
R = distance from Earth's center to spacecraft cm
$\mathbf{r}$ = direction from the cm to an element of volume
$\hat{\mathbf{r}}$ = unit vector in direction of Earth's radius vector
$\mathbf{r}_s$ = radius vector from surface element to spacecraft cm
S = area exposed to sun
$\mathbf{T}_a$ = torque due to aerodynamic pressure
$\mathbf{T}_{EC}$ = torque due to the induced eddy currents
$\mathbf{T}_G$ = torque due to gravity gradient
$\mathbf{T}_{RM}$ = torque due to the residual magnetic moment on spacecraft
$\mathbf{T}_{sp}$ = torque due to solar pressure
T_x,T_y,T_z = body axis components of torque
V_o = spacecraft orbital speed
X_I = inertial X axis directed from Earth's center to the vernal equinox
Y_I = inertial Y axis forming the inertial triad
Z_I = inertial Z axis oriented along the Earth's polar axis
$\alpha_1,\alpha_2,\gamma_1,\gamma_2$ = Euler symmetric parameters
$\Delta\theta$ = deviation of θ due to torque, arc sec; similarly, $\Delta\phi$ and $\Delta\psi$ are due to torque
∇^2 = Laplacian operator
$\nabla\phi$ = gradient of electric potential
ϵ = thickness of solar panels
ϵ_o = reflection coefficient of surface
θ = attitude angle about the second-displaced y axis
μ = Earth's gravitational constant, 1,4082 $\times$ 10^{16} ft^3/sec^2
μ_o = permeability
ρ_a = stream density
σ = static electrical conductivity
τ,L,W = same parameters for the cylinder panels
$\hat{\tau}$ = unit vector directed at sun
τ_B = direction cosines of sun vector in the body frame
τ_x,τ_y,τ_z = torque components divided by I_y
ϕ = attitude angle about the first-displaced x axis
ψ = attitude angle about the inertial Z_I axis
Ω = longitude of the ascending node
ω = spacecraft angular rate vector
$\omega_x,\omega_y,\omega_z$ = component of spacecraft angular rate

Introduction

PRECISE determination of spacecraft attitude is required for infrared measurements for Earth resources detection, military surveillance, and meteorology research. This paper describes an attitude determination system designed for a lifetime of 1 yr and an attitude accuracy of 14-arc sec, as a result of an Attitude-Referenced Radiometer Study (ARRS).† A passive scanned star mapper and a sun mapper on a spin-stabilized vehicle determine transit times of a celestial body, and a ground data reduction program uses the transit times to estimate the spacecraft attitude. A vehicle model including significant environmental torque models is used to extrapolate the vehicle state to the celestial observation time, and at this time the vehicle state is updated. Two requirements are: 1) the model must predict the vehicle state about the spin axis within 14-arc sec between celestial observations and 2) data reduction must be fast enough to prevent any backlogging of data collected throughout the 1 yr period. For the ARRS mission (see Table 1), the disturbance torques caused by eddy currents, residual magnetic moments, solar pressure, aerodynamic pressure, and gravity gradient have been modeled. This paper discusses the torque models. Computer simulations determine the attitude deviation resulting from each torque relative to an untorqued vehicle. Also, the validity of comparing each torque to the untorqued case rather than to the 5-torque case was determined through the use of a torque additive property simulation. Simplifications of the models are made where possible, and suggestions for simplification are noted. Prediction times for various combinations of torque used in the model are given.

Received November 12, 1969; revision received August 31, 1970.

* Principle Systems Analyst, Systems and Research Division.

† The ARRS was conducted by Honeywell Inc. for NASA Langley Research Center under contract NAS1-8801.

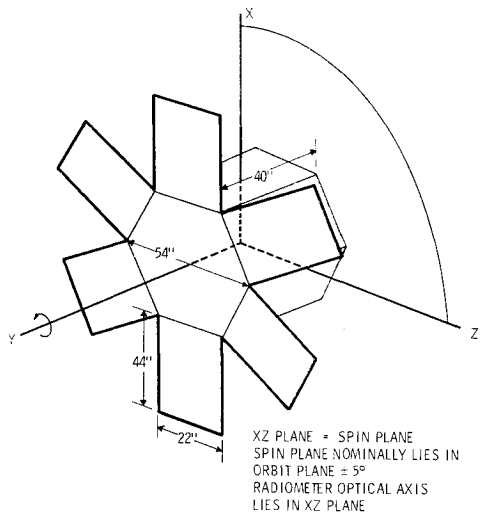

Fig. 1 ARRS spacecraft configuration.

Table 1 ARRS mission requirements and S/C configuration

Orbital parameters: 500 km circular orbit at 97.38° inclination Phasing—3:00 a.m. or 3:00 p.m. for Ω = 45° longitude of the ascending node
Spacecraft configuration (see Fig. 1)
Inertia characteristics: I_y = 65 slug-ft²; $I_x = I_z$ = 54.2 slug-ft²
Magnetic characteristics:
Moment coefficients: $M_x = M_y = M_z = 0$ ($\pm 5 \times 10^{-6}$) ft-lb/Gauss due to preflight compensation uncertainties
ΔM_x due to differences in sunlight and dark conditions = 5% of M_x
Experiment optical axis: lies in spin plane
Operational characteristics
Spin rate: 3 rpm
Attitude: spin axis nominally perpendicular to orbit plane within ±5°; no control applied during instrument measurement period

Torque Models

The computer program computed the attitude for an untorqued vehicle and the attitude and torque for the torqued vehicle. Differences in the attitude and torque for output were then computed. In all the simulation runs, the orbit parameters were identical. The local anomaly ν at the equator and a south heading, longitude of the ascending node Ω, and the inclination i are 187°, 45°, and 97.83°, respectively.

Residual Magnetic Moments

A torque will exist due to the interaction of current flow in the spacecraft electrical circuits and induced moments with the Earth's magnetic field vector **B**. The magnitude of the moment is expected to vary due to changes in spacecraft control modes and power usage. While the design of the spacecraft can reduce the magnitude of the moment, a residual magnetic moment **M** will remain, causing a torque,

$$\mathbf{T}_{RM} = \mathbf{M} \times \mathbf{B} \qquad (1)$$

The $\mathbf{T}_{RM}$ model was programmed, and a 1-orbit simulation was made using the following values of the moments: $M_x = M_y = M_z = 5.170856 \times 10^{-6}$ ft-lb/gauss.

This moment value is representative of the early Tiros spacecraft. Initial conditions were chosen such that a cone angle of 0.61° was obtained, and the principal y axis of the body was misaligned to the orbit normal by ~7.5°. Figure 2 shows T_x, T_y, and $|\mathbf{T}|$ vs time.

The first and second peaks of the envelope of each torque plot represent the south and north pole of the Earth, respectively. At these points, the magnetic field components are greatest in the orbit plane and thus give the largest cyclic variations. The y component of torque is cyclic with a period of 20 sec and a mean value of zero, it is a function of B_x, M_x, M_z, and B_z where M_x and M_z are constants, and B_x and B_z are cyclic in body axes with a 20-sec period due to the spacecraft spin. The x component is also cyclic, with a period of 20 sec (3 rpm spin rate) and with a mean which varies with position in orbit because of the (M_zB_y) term; the cyclic portion is due to the (M_yB_z) term.

The cyclic nature of the torque does not create a cyclic variation in the attitude difference $\Delta\theta$. The deviation in θ at 95 min is −75 arc sec. Although $\Delta\phi$ and $\Delta\psi$ have spin rate

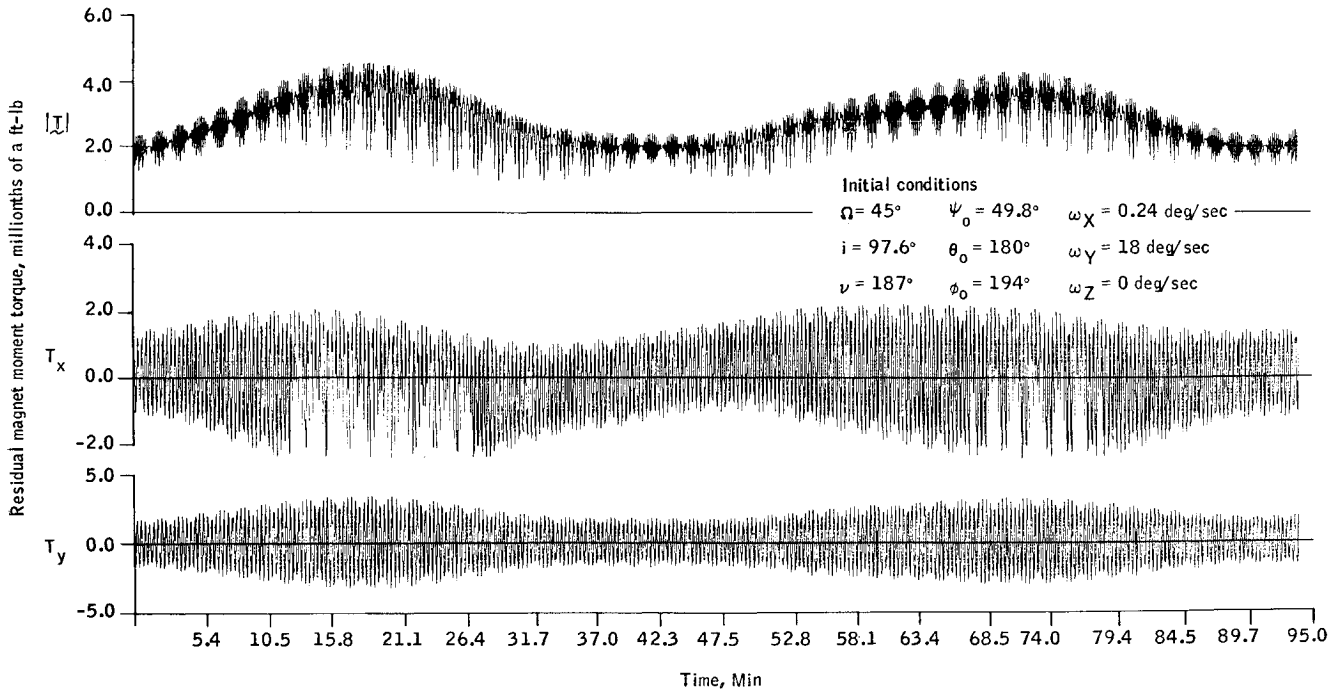

Fig. 2 Torque on spacecraft due to residual magnetic moments.

cyclic variation, the extent of the variation is insignificant over the full orbit ~1 arc sec variation of $\Delta\phi$ at 95 min. These results suggest that short-term variation of torque with a period of 20 sec and mean of zero may be deleted from the torque model. The difference $\Delta\psi$ has orbital variation of ±10-arc sec on a mean drift of 40-arc sec/orbit.

Eddy Currents

Eddy currents are induced in the spacecraft due to the spin motion of the spacecraft. Vinti[1] showed that the interaction of the generated eddy currents and Earth's magnetic field produced a torque that precessed the spin axis of a spherical spacecraft in addition to causing spin decay. For a spherical-conducting spacecraft[1]

$$\mathbf{T}_{EC} = K(\boldsymbol{\omega} \times \mathbf{B}) \times \mathbf{B} \tag{2}$$

where K is a coefficient based on the spacecraft dimensions and conductivity, and $\boldsymbol{\omega}$ is the spacecraft spin vector.

The appealing feature of this model is the single coefficient. In using this model the attitude determination estimation program need estimate only one coefficient. The subject spacecraft configuration, however, is not a sphere, and a new model was derived to determine whether more coefficients are necessary to describe the eddy current effects.

The general expression in gaussian units for the torque on a spacecraft due to eddy current interaction is

$$\mathbf{T}_{EC} = 1/c\int \mathbf{r} \times (\mathbf{J} \times \mathbf{H})dV \tag{3}$$

where $\mathbf{J}$ is the volume eddy current density, $\mathbf{r}$ is the direction from the cm to the element of volume, c is the speed of light in vacuum, $\mathbf{H}$ is the Earth's magnetic field strength $= \mathbf{B}/\mu_o$, and μ_o is the permeability $= 1$ for aluminum.

The volume current density in closed form is given by[2]

$$\mathbf{J} = \tfrac{1}{2}\sigma^{-1}(\boldsymbol{\omega} \times \mathbf{H}) \times \mathbf{r} + \nabla\phi$$

where σ is the static electrical conductivity, and ϕ is the potential that is required to satisfy the boundary condition and LaPlace equation $\nabla^2\phi = 0$. For a sphere, ϕ is a constant and $\nabla\phi = 0$. The solution is now easily obtained for the sphere by integrations over the volume.

For the ARRS configuration, $\mathbf{J}$ was derived for the skin of the spacecraft, assuming that each solar panel and the cylinder sides are electrically isolated, and the skin was chosen to be thin, thus reducing $\mathbf{J}$ to a two-dimensional problem. First, the $\mathbf{J}$ in the rectangular panel must be computed in closed form. Thus, $\mathbf{J}$ is known once ϕ is known. Then ϕ is determined by the boundary conditions that currents normal to the boundary are zero, and LaPlace's equation. This boundary-value problem is the Neumann-type for which very few closed-form solutions are known. However, for the two-dimensional case with simply connected regions, the Neumann problem can be reduced to the Dirichlet problem by using the Cauchy-Riemann[3] conditions, which transform ϕ into stream function ψ. Following this procedure, solutions for the stream functions are obtained, and the torque integral is rephrased in terms of the stream function before integration. The torque expression is obtained by integration over the volume of each panel relative to a common body axis frame and adding all torque due to each panel. Carrying out the integration, the closed-form torque equation for the ARRS configuration is:

$$\begin{aligned}
T_{EC_x} &= -p_1(\omega_x H_y^2 - \omega_y H_x H_y) - p_2(\omega_x H_z^2 - \omega_z H_x H_z) \\
T_{EC_y} &= p_3[\omega_y(H_x^2 + H_z^2) - \omega_x H_x H_y - \omega_z H_y H_z] \\
T_{EC_z} &= -p_1(\omega_z H_y^2 - \omega_y H_y H_z) - p_2(\omega_z H_x^2 - \omega_x H_x H_z)
\end{aligned} \tag{4}$$

where the p's are constants evaluated using the dimensions and conductivity of the cylinder panels and solar panels.

The equations for the p's are:

$$\begin{aligned}
p_1 = \Bigg\{ & \frac{1}{2}\sigma c^{-2}\tau W L^3 + \frac{1}{8}\sigma c^{-2}\tau L W^3 - \frac{3}{4}\sigma c^{-2}\tau L_1 L^2 W + \\
& \frac{3}{2}\sigma c^{-2}\tau L W\left(L_1 L - \frac{L^2}{2}\right) - 12\sigma c^{-2}\tau W^2\left(L_1 L - \frac{L^2}{2}\right) \times \\
& \sum_{n=1}^{\infty}\left(\frac{1}{m\pi}\right)^3 A - 24\sigma c^{-2}\tau W^4 \sum_{n=1}^{\infty}\left(\frac{1}{m\pi}\right)^5 A \\
p_2 = \Bigg\{ & -3\sigma c^{-2}\epsilon a d h^2 - \frac{9}{8}\sigma c^{-2}\epsilon d h^3 - \frac{1}{8}\sigma c^{-2}\epsilon d^3 h \times \\
& 24\sigma c^{-2}\epsilon d^2\left(ah + \frac{h^2}{2}\right)\sum_{n=1}^{\infty}\left(\frac{1}{m\pi}\right)^3 B - \\
& 48\sigma c^{-2}\epsilon d^4 \sum_{n=1}^{\infty}\left(\frac{1}{m\pi}\right)^5 B \\
p_3 = \Bigg\{ & -\frac{3}{8}\sigma c^{-2}\tau W^3 L - \frac{3}{8}\sigma c^{-2}\tau W L^3 - \frac{9}{4}\sigma c^{-2}\tau W L \times \\
& \left(L_1 L - \frac{L^2}{2}\right) + 36\sigma c^{-2}\tau W^2\left(L_1 L - \frac{L^2}{2}\right)\sum_{n=1}^{\infty}\left(\frac{1}{m\pi}\right)^3 A + \\
& 72\sigma c^{-2}\tau W^4 \sum_{n=1}^{\infty}\left(\frac{1}{m\pi}\right)^5 A
\end{aligned} \tag{5}$$

where $A = \tanh(m\pi L/2W) + (L/W)^4 \tanh(m\pi W/2L)$, $B = \tanh(m\pi h/2d) + (h/d)^4 \tanh(m\pi d/2h)$, and ϵ, h, and d are the thickness, length, and width, respectively, of solar panels; τ, L, and W are the same parameters for cylinder panels; $m = 2n - 1$, where $n = 1,2,3, \ldots$; $a = 3^{1/2}W/2$; and $L_1 = L - L_2 =$ distance from cm to end of cylinder opposite solar panel end.

The torque expression has three coefficients for the ARRS configuration spacecraft as compared to the single coefficient for the spherical configuration. The coefficients (p_1,p_2,p_3) evaluated using the baseline dimensions of the vehicle and a static conductivity of aluminum at 20°C[1] are 2.075×10^{-6}, 7.20×10^{-5}, and 6.226×10^{-6} ft-lb-sec/G^2, respectively.

The coefficient p_3 was chosen to be the same as the spherical model coefficient K and p_1 and p_2 were scaled in proportion to the foregoing computed values. Figure 3 is a plot of the ARRS configuration torque using the computed coefficients for a one-half orbit simulation. The y component varies only as a function of orbit position; however, the x component varies at the spin frequency and the spin vector precession frequency (motion of $\boldsymbol{\omega}$ in the body). The peak points of the torque occur at the poles because of the greater magnitude of the field at the poles.

There is no cyclic variation of $\Delta\theta$, but $\Delta\psi$ and $\Delta\phi$ possess a spin-rate cyclic variation. The deviation in $\Delta\theta$ at 45 min is 3500-arc sec, and $\Delta\phi$ and $\Delta\psi$ have a peak-to-peak variation of 37.5-arc sec. The results suggest, for accurate propagation of spacecraft attitude, that the torques caused by eddy currents be included in the vehicle dynamics.

It is of interest to simplify the new model by reducing the number of coefficients required to be estimated. A computer simulation was conducted computing the difference in attitude generated by the two models. The differences of the two models are 1.4 arc sec in $\Delta\theta$ at 45 min, and 0.4-arc sec peak-to-peak in $\Delta\psi$ about a zero mean at 45 min. For the attitude determination accuracy considered, the spherical model is adequate for the attitude determination algorithm.

Electromagnetic Radiation

The intensity of electromagnetic radiation is inversely proportional to the square of the distance from the sun. About 99% of this solar energy lies in the narrow band from 3000 to 4000 Å,[4] with the remaining 1% distributed in the ultraviolet, infrared and radio frequencies. The incident electromagnetic radiation power density (the solar constant) received outside the Earth's atmosphere at 1 a.u. from the sun is 1396 ±

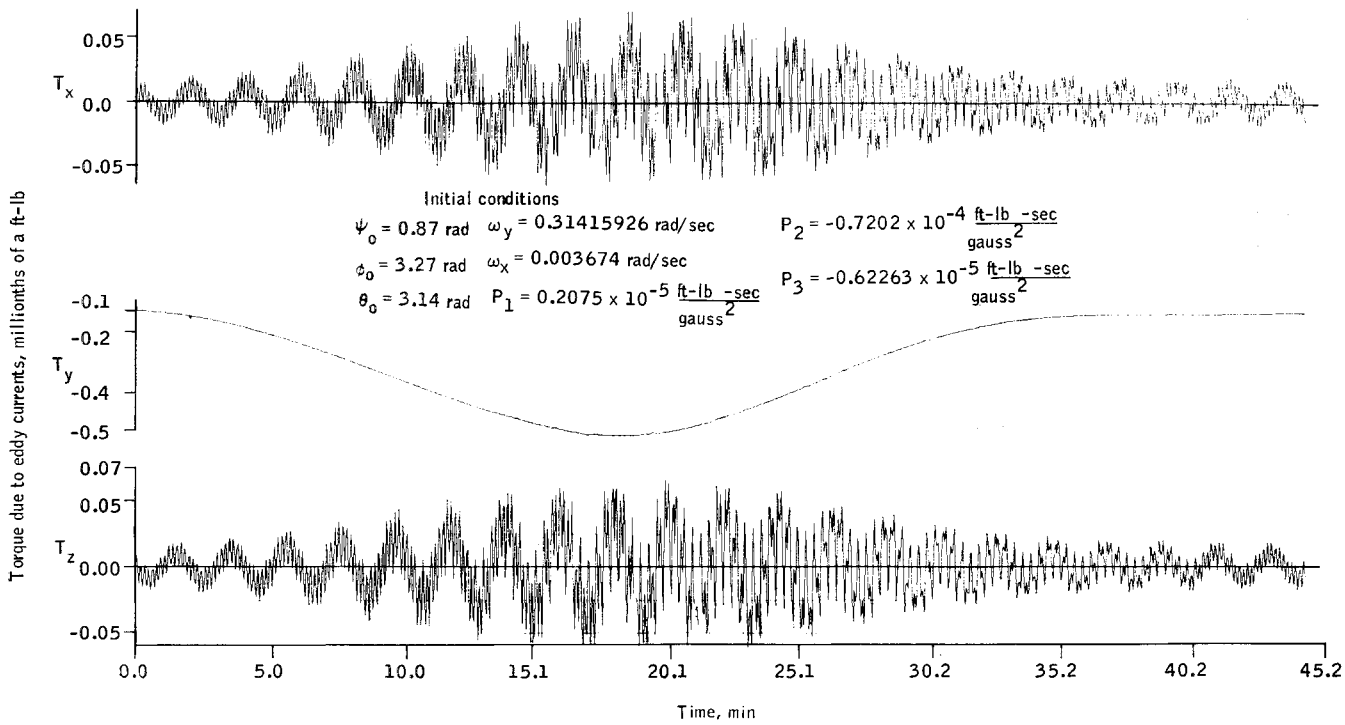

Fig. 3 Torque on spacecraft due to induced eddy currents.

14 w/m². This power density which produces "light pressure" is virtually unchanged with high solar activity. The radiation pressure P_e acting on a nonreflective surface normal to the incoming radiation

$$P_e = E_0/c = 4.636 \times 10^{-6} \text{N/m}^2$$

where E_0 = solar constant (1396 w/m²).

In developing the solar pressure disturbance torque model, a constant pressure $P_e = 1 \times 10^{-7}$ lb/ft² is used for a surface normal to the sun line with no variation due to solar activity. The torque is computed from the following three formulas taken from Beletskii[6]

$$\mathbf{m}^+ = \tilde{\tau} \times \int_{s_1} \mathbf{r}_s(\tilde{n}\cdot\tilde{\tau})ds \tag{6}$$

$$\mathbf{m}^- = 2\int_{s_1} \tilde{n} \times \mathbf{r}_s\,(\tilde{n}\cdot\tilde{\tau})^2 ds \tag{7}$$

$$\mathbf{T}_{sp} = P_e[(1-\epsilon_0)\mathbf{m}^+ + \epsilon_0 \mathbf{m}] \tag{8}$$

where ds = an area differential, $\mathbf{r}_s$ = vector from body's c.m. to ds, $\hat{\tau}$ = unit vector directed from sun, $\hat{n}$ = unit outward normal to ds, and ϵ_0 = body's reflection coefficient.

The integrations described in Eqs. (6) and (7) are performed over the sun-exposed surfaces of the spacecraft. Three assumptions are made about the exposed surfaces: 1) the sun never shines on the end of the spacecraft opposite the solar panels; 2) the shadow of the tip of a solar panel never strikes any part of the spacecraft; and 3) the sides of the spacecraft (i.e., not the solar panels) constitute a circular cylinder rather than a hexagonal one. The integrations of Eqs. (6) and (7) over the end solar panels are quite simple; the integrations over the sides are considerably more complicated. Since this end of the spacecraft is always fully illuminated, integration of Eqs. (6) and (7) is performed to obtain a closed form for

$$\mathbf{m}^+ = \begin{bmatrix} -c_o b_o L_2 S \\ 0 \\ a_o b_o L_2 S \end{bmatrix}, \quad \mathbf{m}^- = \begin{bmatrix} 0 \\ 0 \\ 0 \end{bmatrix}$$

$$\tau_B = \begin{bmatrix} a_o \\ b_o \\ c_o \end{bmatrix} = \text{direction cosines of sun vector in the body frame}$$

L_2 = length from c.m. to the solar panel end

S = area exposed to the sun

The integration over the cylinder portion of the spacecraft is more complicated than the solar panels because shadows are created on the cylinder by the solar panels. The solution over the cylinder portion consists of integration over the cylinder area with shadowing taken into account. The sunlight passes between two solar panels to expose a portion of the cylinder. This occurs between all panels if the surface is normal, $\hat{n} < 90°$ to the sun line. The equations for $\mathbf{m}^+$ and $\mathbf{m}^-$ are integrated to obtain an analytical form for exposure of the cylinder for light passing between two panels. The result for $\mathbf{m}^+ = \int(\hat{n}\cdot\hat{\tau})ds$ is, for the $\hat{i}$ component

$$K_1' r_3 \left\{ \frac{-d3^{1/2}}{3} a_o \cos\theta(\sin^2\theta + 2) + (dc_o 3^{1/2} - a_o)\frac{\sin^3\theta}{3} + \frac{c_o}{3}\cos^3\theta \right\} + r_3(K_1' + L)\left\{ \frac{a_o}{2}(\theta - \sin\theta\cos\theta) + \frac{c_o}{2}\sin^2\theta \right\}\Bigg|_{\Phi_1}^{\Phi_2}$$

For the $\hat{j}$ component

$$K_1'^2 \left\{ -\frac{a_o}{3}\cos\theta(\sin^2\theta + 2) + (c_o - d3^{1/2}a_o)\frac{\sin^3\theta}{3} + \frac{d3^{1/2}c_o}{2}\cos^3\theta \right\} + K_1(K_1 + L_2)\left\{ \frac{d3^{1/2}a_o}{2}(\theta - \sin\theta\cos\theta) + (d3^{1/2}c_o - a_o)\frac{\sin^2\theta}{2} - \frac{c_o}{2}(\theta + \sin\theta\cos\theta) - a_o\cos\theta + c_o\sin\theta \right\} - L\left(\frac{L}{2} - L_2\right)(-a_o\cos\theta + c_o\sin\theta)\Bigg|_{\Phi_1}^{\Phi_2}$$

For the $\hat{k}$ component

$$K_1 r_3 \left\{ \frac{da_o 3^{1/2}\sin^3}{3}\theta + (a_o - d3^{1/2}c_o)\frac{\cos^3\theta}{3} - \frac{c_o}{3}\sin\theta \times (\cos^2\theta + 2) \right\} + r_3(K_1 + L)\left\{ \frac{a_o}{3}\sin\theta + \frac{c_o}{2} \times (\theta + \sin\theta\cos\theta) \right\}\Bigg|_{\Phi_1}^{\Phi_2}$$

The result for

$$\mathbf{m}^- = \iint_S \hat{n} \times \hat{r}_s(\hat{n}\cdot\hat{\tau})^2 dA$$

is, for the $\check{\mathbf{i}}$ component

$$-K_1^2\left\{\frac{a_o}{5}\sin^5\theta + (2a_oc_o - d3^{1/2}a_o^2)\left[\frac{1}{5}\sin^4\theta\cos\theta - \frac{1}{15}\cos\theta(\sin^2\theta + 2)\right] + (c_o^2 - 2d3^{1/2}a_oc_o)\left(\frac{1}{5}\sin^3\theta\cos^2\theta + \frac{2}{15}\sin^3\theta\right) + \frac{d3^{1/2}}{5}c_o^2\cos^5\theta\right\} - K_1(K_1 + L_2)\times$$

$$\left\{\frac{d3^{1/2}}{4}a_o^2\sin^4\theta + \frac{1}{8}(2d3^{1/2}a_oc_o - a_o^2)\left(\theta - \frac{1}{4}\sin_4\theta\right) - \frac{1}{4}(d3^{1/2}c_o^2 - 2a_oc_o)\cos^4\theta - c_o^2\left[\frac{1}{4}\sin\theta\cos^3\theta + \frac{3}{8}\times(\theta + \sin\theta\cos\theta)\right] + \frac{a_o^2}{3}\sin^3\theta - \frac{2}{3}a_oc_o\cos^5\theta + \frac{c_o^2}{3}\times\right.$$

$$\left.\sin\theta\,(\cos^2\theta + 2) + L\left(\frac{L}{2} - L_2\right)\left[\frac{a_o^2}{3}\sin^3\theta - \frac{2}{3}a_oc_o\cos^3\theta + \frac{c_o^2}{3}\sin\theta\,(\cos^2\theta + 2)\right]\right|_{\Phi_1}^{\Phi}$$

For the $\hat{\mathbf{j}}$ component, zero, and for the $\hat{\mathbf{k}}$ component

$$K_1^2\left\{a_o^2\left[-\frac{1}{5}\sin^4\theta\cos\theta - \frac{4}{15}\cos\theta(\sin^2\theta + 2)\right] + \frac{1}{5}\times(2a_oc_o - d3^{1/2}a_o^2)\sin^5\theta + (c_o^2 - 2d\,3a_oc_o)\left[\frac{1}{5}\sin^4\theta\cos\theta - \frac{1}{15}\cos\theta(\sin^2\theta + 2)\right] + -d\,3^{1/2}c_o^2\left(\frac{1}{5}\sin^3\theta\cos^2\theta + \frac{2}{15}\sin^3\theta\right)\right\} + K_1(K_1 + L_2)\left\{d3^{1/2}a_o^2\left[\frac{1}{4}\sin^3\theta\cos\theta + + \frac{3}{8}(\theta - \sin\theta\cos\theta)\right] + \frac{1}{4}(2d3a_o^{1/2}c_o - a_o^2)\sin^4\theta + \frac{1}{8}(d3^{1/2}c_o^2 - 2a_oc_o)\left(\theta - \frac{1}{4}\sin4\theta\right) + \frac{c_o^2}{4}\cos^4\theta - \frac{1}{3}\times a_o^2\cos\theta\,(\sin^2\theta + 2) + \frac{2}{3}a_oc_o\sin^3\theta + -\frac{c_o^2}{3}\cos^3\theta - L\times\left(\frac{L}{2} - L_2\right)\left[-\frac{a_o^2}{3}\cos\theta(\sin^2\theta + 2) + \frac{2}{3}a_oc_o\sin^3\theta - \frac{c_o^2}{3}\cos^3\theta\right]\right|_{\Phi_1}^{\Phi^2}$$

where θ is a dummy variable evaluated between limits Φ_1 and Φ_2, K_1 is an integration parameter, and L is the length of the cylinder.

This solution is true, in general, for light passing between any two solar panels. The numerical evaluation can be completed for the value of the torque at any instant, given Φ_1 and Φ_2, which are functions of the sun-line direction cosines and surface orientation relative to the body-fixed axes and are determined at each evaluation time. In the computer simulations of flights, real time seldom exceeds 2 or 3 hr, and it will be assumed that S is a constant. A computer subprogram for $\mathbf{T}_{sp}$ is called at each time step of the numerical integration of the equations of motion of the spacecraft. It should be emphasized that the integrations of Eqs. (6) and (7) are not performed numerically but are evaluated analytically at each time step.

A simulation of one-half orbit was performed. The x and y components of the torque (Fig. 4) exhibit cyclic variations. However, the y component is 20 times smaller than the x component. The envelope of the x component torque is essentially constant over the simulation time, indicating very little dependency on orbit position. The peak-to-peak of the x component is symmetric about zero, but Fig. 4 does not show this due to sampling points being 4.8 sec apart. Fig. 5 shows the cyclic variation clearly. The magnitude of the torque is essentially constant over the simulation period at 2.75×10^{-6} ft-lb.

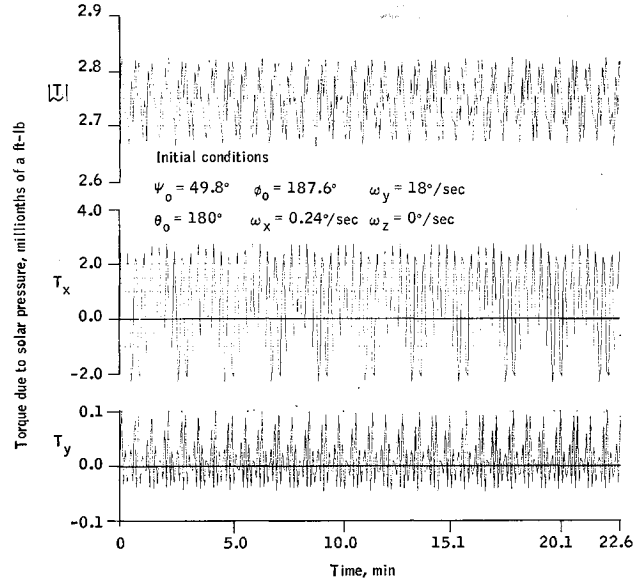

Fig. 4 Torque on spacecraft due to solar pressure.

The deviations in attitude relative to the untorqued vehicle exhibit only slight variation at the spin frequency. Again, this suggests that terms in the torque expression that are cyclic may be deleted from the model. The torque causes a spinup of the vehicle which results in a $\Delta\theta$ of 100-arc sec at 45 min. The angles ϕ and ψ deviate positively from the untorqued case and are +65 and +10 arc sec, respectively, at 45 min. These deviations appear linearly as a function with time, except for $\Delta\theta$ which is increasing nonlinearly.

The $\mathbf{T}_{sp}$ subprogram was slow in execution due to evaluation over the spacecraft cylinder to account for the shadowing and is required at each evaluation step. Three approaches to remedy the execution time were considered: 1) remove the effect of cylinder torque and consider only torque due to solar panels; 2) compute and store torque due to spacecraft shadowing for one or two spin periods; and 3) compute torque due to solar panels normally and add cylinder torque based on the store of torque data for all subsequent scans. Approach 1 was tried unsuccessfully; approach 2 was successful.

Comparing the results at 45 min, the modified program gives $\Delta\theta$ = +97.2-arc sec, $\Delta\phi$ = +74.0-arc sec, and $\Delta\psi$ =

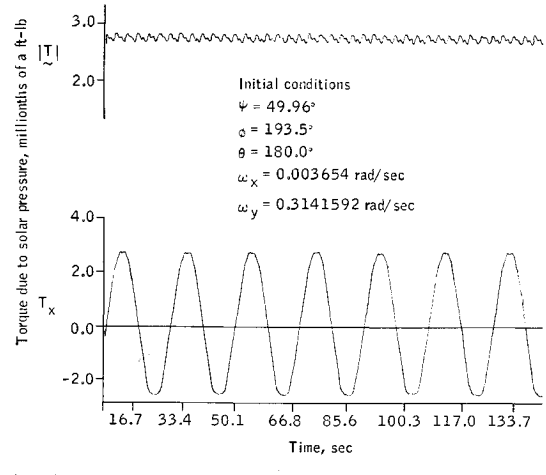

Fig. 5 Torque on spacecraft due to induced eddy currents.

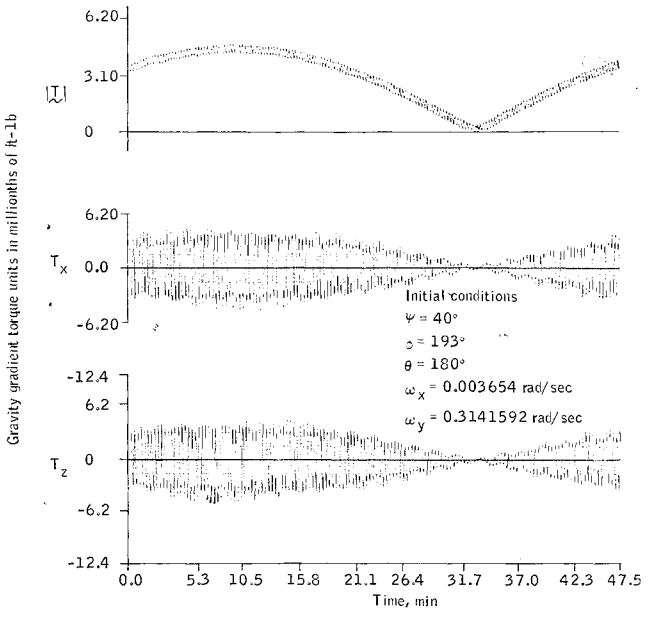

Fig. 6 Torque on spacecraft due to gravity gradient.

+10.0-arc sec with a 1.25-arc sec variation, and the correct model gives $\Delta\theta = +100$-arc sec, $\Delta\phi = +67.5$-arc sec, and $\Delta\psi = +9.0$-arc sec with a 1.25 arc sec variation at the spin frequency. Based on these results, the modified program is sufficiently accurate for simulation periods of $\frac{1}{2}$ orbit, and has been used in subsequent analysis.

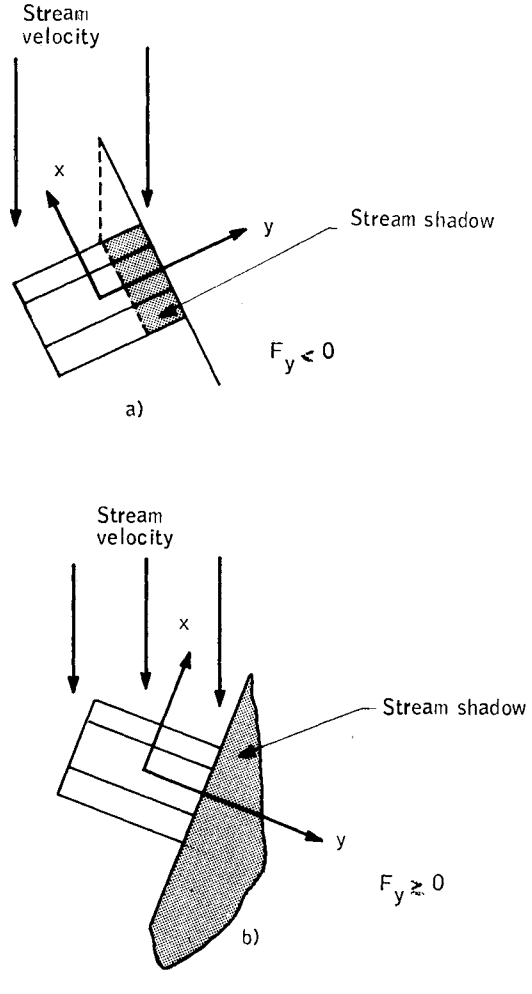

Fig. 7 Aerodynamic stream shadow on spacecraft.

Gravity Gradient

The equations for the gravity gradient are expressed in a body-fixed axes system (principal body axes). The torque on a rigid body caused by the gravity gradient is

$$\mathbf{T}_G = 3\mu\hat{\mathbf{r}} \times \bar{\bar{I}}\cdot\hat{\mathbf{r}}/R^3 \tag{9}$$

assuming that the Earth is spherical. Further, μ = Earth's gravitational constant = 1.4082×10^{16} ft^3/sec^2, $\mathbf{r}$ = unit vector in direction of Earth's radius vector, R = distance from Earth's center to body's c.m., and $\bar{\bar{I}}$ = moment of inertia of the body. In body coordinates, the equations are

$$\begin{bmatrix} T_{Gx} \\ T_{Gy} \\ T_{Gz} \end{bmatrix} = \frac{3\mu}{R_3} \begin{bmatrix} (I_z - I_y)r_{By}r_{Bz} \\ (I_x - I_z)r_{Bz}r_{Bx} \\ (I_y - I_x)r_{Bx}r_{By} \end{bmatrix} \tag{10}$$

where r_{Bx}, r_{By}, and r_{Bz} are the direction cosines of $\hat{\mathbf{r}}$.

A complete orbit simulation was conducted; Fig. 6 is a plot of the torque. For symmetric spacecraft as we have chosen here, $T_{Gy} = 0$. The x and z components of $\mathbf{T}_G$ are cyclic and are the same except they are 90° out of phase. Two zero torque points occur because the spacecraft principal moment of inertia is normal to the orbit plane twice per orbit. The magnitude of $\mathbf{T}_G$ is 4.65×10^{-6} ft-lb, which is slightly higher than the other 4 torques.

The attitude deviation caused by this torque does possess variation at the spin frequency but has only a peak-to-peak variation of 2.5-arc sec in $\Delta\theta$ at 56.3 min and is growing with time. The torque terms that create the attitude variation of the spin frequency may be eliminated considering the attitude accuracy of 14 arc sec. The torque does cause a negative deviation in attitude, θ, ϕ, and ψ are -17-, -69-, and -62-arc sec, respectively. The torque affects precession of the spacecraft ϕ and ψ more than spin decay θ. Even for the relatively large value of the torque magnitude, the deviation in attitude is not correspondingly larger than the deviation due to the other torques. This is due to the attenuation of cyclic torque at spin frequencies.

Aerodynamic Torque

The torque $\mathbf{T}_a$ consists of aerodynamic pressure torque due to the spacecraft's center of mass velocity and a dissipative torque due to the spacecraft's angular rate. The torque equation including these two effects is taken from Beletskii's work.[6] The following equation is valid when the spacecraft's orbit velocity is large compared with the rotation of the atmosphere (Earth's rate approximately), the linear surface velocities due to the spin of the satellite is small compared with the spacecraft's center of mass velocity, and the angle of attack of each surface encountered is less than $\pi/2$.

$$\mathbf{T}_a = \tfrac{1}{2}c\rho_a V_o^2 \int (\hat{\mathbf{n}}\cdot\hat{\mathbf{e}}_v)(\hat{\mathbf{e}}_v \times \mathbf{r}_s)ds + \tfrac{1}{2}c\rho_a V_o \int \{(\hat{\mathbf{n}}\cdot[\boldsymbol{\omega} \times \mathbf{r}_s])(\hat{\mathbf{e}}_v \times \mathbf{r}_s) + (\hat{\mathbf{n}}\cdot\hat{\mathbf{e}}_v)[\boldsymbol{\omega} \times \mathbf{r}_s] \times \mathbf{r}_s\}ds \; S(\hat{}\cdot\hat{\mathbf{e}}_v > 0) \tag{11}$$

where $\hat{\mathbf{e}}_v = V_o/|V_o|$. The first term of Eq. (11) represents torque due to misalignment of spacecraft c.m. and c.p. (center of pressure). The second term represents dissipative torque due to spacecraft spin. Upon examining the coefficient of each term, the torque due to c.p. misalignment is approximately a factor of V_o larger than the dissipative torque coefficient when $\omega r \ll V_o$. For a 500 km-altitude orbit, V_o is 2.624×10^4 ft/sec.

Dissipative torque is a factor of 10^4 less than pressure torque and is sufficiently small that the second term of Eq. (11) will

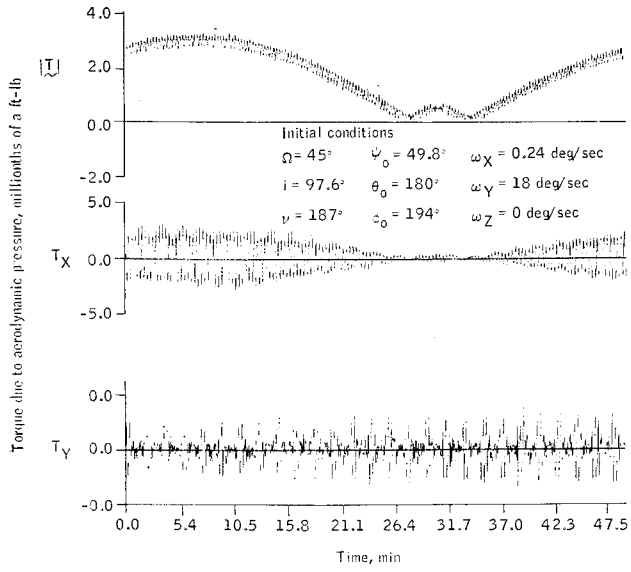

Fig. 8 Torque on spacecraft due to aerodynamic pressure.

be neglected. Then

$$\mathbf{T}_a = \tfrac{1}{2}C\rho_a V_o^2 \int (\hat{\mathbf{n}}\cdot\hat{\mathbf{e}}_v)(\hat{\mathbf{e}}_v \times \mathbf{r}_s)\,ds\, S(\hat{\mathbf{n}}\cdot\mathbf{e}_v > 0) \qquad (12)$$

where domain of integration is indicated by $S(\mathbf{n}\cdot\hat{\mathbf{e}}_v > 0)$.

The direction of the stream is in the orbit plane, and for this reason the spacecraft will present a different surface to the stream, depending on the attitude of the vehicle.

Figure 7 illustrates two orientations of the spacecraft that give two different domains for Eq. (12). The aerodynamic torque will be represented by two equations because of the different surfaces presented to the stress as shown in Fig. 7. The torque equation for the solar panels when $F_y \geq 0$ is given by Eq. (12) where $S(\hat{\mathbf{n}}\cdot\hat{\mathbf{e}}_v) > 0$ is the exposed area in Fig. 7b.

Torque due to aerodynamic pressure for $F_y < 0$ is different than for $F_y > 0$ (Fig. 7b). The solar panels are not shadowed, but the cylinder is as shown in Fig. 7a. The shadow, however, on the cylinder will be limited due to the attitude control limits.

In the derivation of the torque for the solar panels, we assume a solid disk, where in actuality there are six rectangular panels (Fig. 1).

Summarizing the equations for the torque, one has

$$\mathbf{T}_a = \begin{cases} q_2\hat{\mathbf{e}}_v \times \left[\sum_i (\hat{\mathbf{n}}_1\cdot\hat{\mathbf{e}}_v)\mathbf{v}_1 + (\mathbf{n}\cdot\hat{\mathbf{e}}_v)(\mathbf{v}+\mathbf{v}_E)\right] \\ \qquad\qquad \text{for } \hat{\mathbf{e}}_v\cdot\hat{\mathbf{j}} \leq 0 \text{ or } F_y \geq 0 \\ (\mathbf{n}_i\cdot\hat{\mathbf{e}}_v > 0) \\ q_2\hat{\mathbf{e}}_v \times \left[\sum_i (\mathbf{n}\cdot\hat{\mathbf{e}}_v)\mathbf{v}_1 + (\hat{\mathbf{n}}'\cdot\hat{\mathbf{e}}_v)\mathbf{v}'\right] \\ \qquad\qquad \text{for } \hat{\mathbf{e}}_v\cdot\hat{\mathbf{j}} > 0 \text{ or } F_y < 0 \\ (\hat{\mathbf{n}}_i\cdot\hat{\mathbf{e}}_v > 0) \end{cases}$$

where

$$\mathbf{v}_i = \frac{3^{1/2}}{2} W^3 L \cos\frac{\pi}{3}(i-1)\hat{\mathbf{i}} + \frac{W}{2}(L_2^2 - L_1^2)\hat{\mathbf{j}} - \frac{3}{2} W^3 \sin\frac{\pi}{3}(i-1)\hat{\mathbf{k}}$$

$$\hat{\mathbf{n}}_i = \cos\tfrac{\pi}{3}(i-1)\hat{\mathbf{i}} - \sin\tfrac{\pi}{3}(i-1)\hat{\mathbf{k}} \text{ for } i = 1, \ldots 6.$$

$$\mathbf{n} = -\hat{\mathbf{j}}, \quad \hat{\mathbf{n}}' = \hat{\mathbf{j}}$$

$$\mathbf{v}_i' = \frac{3}{2} W^3(L_1 + L_2')\cos\frac{\pi}{3}(i-1)\hat{\mathbf{i}} + \frac{W}{2}(L_2'^2 - L_1^2)\hat{\mathbf{j}} - \frac{3W^3}{2}(L_1 + L_2')\sin\frac{\pi}{3}(i-1)\hat{\mathbf{k}}$$

$$L_2 = [L_2' - (r_4 - r_3)(\hat{\mathbf{e}}_v\cdot\hat{\mathbf{j}})]/[1 - (\hat{\mathbf{e}}_v\cdot\hat{\mathbf{j}})^2]^{1/2}$$

$$\mathbf{v}' = L_2\pi(r_4^2 - r_3^2)\hat{\mathbf{j}}, \quad \mathbf{v}_E = L_1\pi r_3^2\mathbf{j}$$

$$\mathbf{v} = [r_3(r_4^2 - r_3^2)\sin\theta]\hat{\mathbf{i}} + \left[L_2\pi r_4^2 - L_2\pi r_3^2 - L_2 r_3(r_4^2 - r_3^2)^{1/2} - L_2 r_4^2 \sin^{-1}\left(\frac{r_3}{r_4}\right)\right]\hat{\mathbf{j}} - [r_3(r_4^2 - r_3^2)\cos\theta]\,\hat{\mathbf{k}}$$

where $\sin\theta = v_x/(1 - v_y^2)^{1/2}$, $\cos\theta = v_z/(1 - v_y^2)^{1/2}$, and v_x, v_y, and v_z are the components of the $\hat{\mathbf{e}}_v$ vector in body axes and the symbol $(\mathbf{n}_i\cdot\hat{\mathbf{e}}_v > 0)$ means sum over the surfaces whose angle of attack is positive.

Table 2 Summary of attitude deviations $\Delta\theta$ and $\Delta\phi$ (arc sec) due to each torque and the total torque vs the sum of the five

Time, min	Residual magnetic moment	Eddy current	Gravity gradient	Aerodynamic pressure	Solar pressure	Total	Sum, 1–5
				$\Delta\theta$, arc sec			
5	−5.9	−20.6	+0.24	−0.02	+1.6	−24.2	−24.7
10	−10.6	−98.7	−0.97	−0.06	+6.4	−102.0	−102.0
15	−15.0	−269.1	+1.40	−0.44	+14.2	−268.8	−268.9
20	−19.3	−566.8	+1.50	−0.69	+24.4	−560.8	−560.9
25	−23.1	−1000.6	+2.00	−0.24	+38.6	−983.3	−983.3
30	−27.5	−1536.4	+1.20	−0.56	+55.1	−1508.1	−1508.2
35	−32.4	−2144.5	+1.08	−0.44	+74.1	−2101.8	−2102.2
40	−37.3	−2792.8	+1.17	−0.31	−97.9	−2730.7	−2730.7
45	−42.6	−3473.9	+0.10	+0.52	+122.6	−3394.4	−3393.3
				$\Delta\phi$, arc sec			
5	+2.8	−0.17	+7.0	+0.25	+8.0	+18.0	+17.9
10	+8.4	−0.04	+11.7	+1.1	+16.3	+37.0	+37.5
15	+14.2	+2.1	+13.0	+2.6	+24.3	−56.5	+56.3
20	+16.9	−5.6	+16.4	+8.7	+32.6	+68.9	+69.0
25	+16.2	+5.8	+13.6	+10.5	+40.8	+87.0	+86.9
30	+12.4	+4.7	+15.0	+14.2	+48.4	+95.2	+95.1
35	+7.8	−22.4	+22.2	+19.9	+57.4	+84.8	+84.9
40	+4.3	+28.1	+21.3	+14.7	+64.7	+133.3	+133.1
45	+0.6	−10.8	+33.0	+18.4	+73.5	+114.7	+115.7

The torque due to the solar panels in reality is varying with a frequency six times the spin rates as opposed to the result obtained in this analysis. This is because the shaded area covers only part of the two solar panels, and as the spacecraft rotates, varying amounts of solar panel area are shaded. The disk-shaped panels give a larger magnitude of torque but remain constant in absolute value.

A simulation of one full orbit was made and the torque is shown in Fig. 8. The magnitude of the torque varies with position in orbit, ranging from 0 to 3.0×10^{-6} ft-lb. The x component is cyclic at the spin frequency and possesses two periods of nulls over one orbit when the angle of attack is near zero. Because spacecraft is spin stabilized, the angle of attack will become zero twice. The y component of torque is zero.

The deviation of the attitude due to this torque is bounded over one orbit. The deviation of $\Delta\theta$ reaches -5 arc sec at 20 min and remains constant to 36.7 min, then it reaches $+2.0$-arc sec at 65 min. The attitude angles are bounded within $+10$ and -20 arc sec for $\Delta\psi$ and within $+25$- and $+5$-arc sec for $\Delta\phi$. The aerodynamic torque indicates greater effect on the precession of the angular momentum vector than in the spin decay. The cyclic variation at the spin frequency is at most 2.5-arc sec peak-to-peak. This suggests that cyclic terms of the torque model can be dropped.

Torque Model Additive Property

For the purposes of simplifying the vehicle model used in an attitude estimation algorithm, prediction times for various combinations of torque must be determined. An analysis was conducted to show that the individual effects (i.e., the attitude deviation due to the individual torques relative to an untorqued spacecraft) of each of the five torques can be summed to give the same effect as the combined five torques. Table 2 show that $\Delta(\Delta\theta)$ is approximately 1.1-arc sec after 45 min of orbit. This number could very well be attributed to round-off (10th and 11th decimal place). The difference in $\Delta(\Delta\phi)$ is at worst 1.0-arc sec over 45 min, and $\Delta(\Delta\psi)$ is at worst 0.5-arc sec. The results demonstrate the additive effect of the torques on the spacecraft attitude. The result allows one to determine quickly the prediction time allowed to meet the specified 14-arc sec accuracy in attitude for various combinations of torques. The residual magnetic moment and eddy currents cause the greatest spin decay ($\Delta\theta$). Solar pressure creates a spin up which reduces the total spin decay. Gravity gradient and solar pressure cause the greatest effect on precession ($\Delta\varphi$).

Table 3 Comparison of the effects of different combinations of torque with the total torque effect on $\Delta\theta$ and $\Delta\phi$ (arc sec)

Time, min	Sum, 1 + 2	Sum, 1 + 2 + 5	Total
	$\Delta\theta$, arc sec		
5	−26.5	−24.9	−24.2
10	−109.3	−102.9	−102.0
15	−284.1	−269.9	−268.8
20	−586.1	−561.7	−560.8
25	−1023.7	−985.1	−987.3
30	−1563.9	−1508.8	−1508.1
35	−2176.9	−2102.8	−2101.8
40	−2830.1	−2732.2	−2730.7
45	−3516.5	−3393.9	−3394.4
	$\Delta\phi$, arc sec		
5	+2.6	+10.6	+18.0
10	+8.4	+24.7	+37.0
15	+16.3	+40.7	+56.5
20	+11.3	43.6	+68.9

Attitude Prediction Time

The prediction time is the time elapsed when the vehicle model attitude propagation for different combinations of torque differs from the five-torque attitude propagation by 14-arc sec. Table 3 lists attitude deviations for various combinations of torque relative to the untorqued case. The last column in each table is the deviation due to the five torques. The deviations in the other columns are compared to the last for determination of the prediction time. Considering θ and ϕ prediction within 14-arc sec, Table 3 shows that the prediction time for ϕ is less than 5 min when only the residual magnetic moment and eddy current models (sum, 1 + 2) are included. By adding solar pressure torque to the model (sum, 1 + 2 + 5), the prediction time can be at least 10 min, based on the five torque model true environment.

Conclusions

The effects of five environmental disturbances on the spacecraft have been determined for the given spacecraft mission. The torques due to the eddy currents, solar pressure and aerodynamic pressure depend on the spacecraft configuration and were derived for the specific spacecraft configuration. The torque due to eddy currents was derived only for the spacecraft skin because the lack of definition of components and packages in the spacecraft. And in general, a closed-form solution for the eddy currents is feasible only for a few special cases. It is concluded that an exact model for the entire source is not feasible. The torques due to solar pressure and aerodynamic pressure were derived in closed form, but due to time-varying shadows in the spacecraft, the closed-form equations are very complex.

The torque due to eddy currents and the residual magnetic moments had the greatest spin decay effect. The gravity gradient torque had the greatest effect on the precession (φ and ψ), i.e., angular momentum precession). The solar pressure created a spin up and was third in its absolute effect on spin. The aerodynamic torque had the least effect on the spacecraft attitude. The five torques were incorporated into a vehicle model that was used in a simulation of the true attitude determination sensor output.[7] For 5-min prediction time between stellar observations, the torques due to the residual magnetic moments and the eddy current are adequate for use in the attitude estimation algorithm to account for spin decay.[7]

By adding the solar pressure to the algorithm model, the spin decay over 45 min is well within the accuracy of 14-arc sec. However, the precession error limits the prediction time to about 10 min using only the magnetic and solar pressure torques.

The ARRS eddy current model was found to have nearly the same effect on attitude as the spherical model. Therefore, the spherical model is adequate for the estimation algorithm. The advantage is that it has one coefficient. This reduces the number of parameters to be estimated and naturally speeds execution of the algorithm which is important when one year of data must be processed. Purely cyclic terms in all of the torques may be removed without loss of state propagation accuracy yet gain speed in program execution. This was shown by E. C. Foudriat.[8] Due to the slow execution time for the solar pressure torque, it was modified to compute the torque due to the time-varying shadows over one spin cycle and interpolated for the entire orbit. The modified model was used in subsequent simulation.[7]

Appendix: Vehicle Model

The equations of motion used to analyze the effect of the torques are

$$\dot{\omega}_x = [\omega_y\omega_z(1 - C) + \tau_x]/A,\ \dot{\omega}_y = \omega_x\omega_z(C - A) + \tau_y$$

$$\dot{\omega}_z = [\omega_x\omega_y(A - 1) + \tau_z]/C,\ \dot{\alpha}_1 = (-\omega_z\alpha_2\,\omega_y\gamma_1 - \omega_x\gamma_2)/2$$

$$\dot{\alpha}_2 = (\omega_z\alpha_1 + \omega_x\gamma_1 + \omega_y\gamma_2)/2,$$
$$\dot{\gamma}_1 = (-\omega_y\alpha_1 - \omega_x\alpha_2 + \omega_z\gamma_2)/2$$
$$\dot{\gamma}_2 = (\omega_x\alpha_1 - \omega_y\alpha_2 - \omega_z\alpha_1)/2$$

where $A = I_x/I_y$ and $C = I_z/I_y$; $\hat{\tau}_x$, $\hat{\tau}_y$, and τ_z are torques divided by I_y; ω_x, ω_y, and ω_z are body rates; and α_1, α_2, γ_1, and γ_2 are Euler symmetric parameters.

The two major coordinate systems used in this program are the inertial coordinate frame and the body-fixed coordinate frame. The inertial coordinate frame has its origin at the center of the Earth with the X_I axis directed to the vernal equinox, and the Z_I axis along the Earth polar axis. The body frame has its origin at the cm, and the axes defined by the principal-moment-of-inertia axes. The Euler angle rotations from the inertial to the body frame are ψ about the Z_I axis, ϕ about the first-displaced x axis, and θ about the second-displaced y axis.

The equations of motion are written in terms of Euler symmetric parameter. Conversion between Euler angles and the symmetric parameter is accomplished by equating the transformation matrix $E(\psi,\phi,\theta)$ to $E(\alpha,\alpha_2,\gamma_1,\gamma_2)$.

The equations of motion were programmed to compute body rates and spacecraft Euler angle attitude for the untorqued case and the specified torque case. The torque in body axes and the difference in Euler angle attitude was plotted.

References

[1] Vinti, J. P., "Theory of the Spin of a Conducting Satellite in the Magnetic Field of the Earth," Rept. 1020, July 1957, Ballistic Research Labs., Aberdeen Proving Ground, Md.

[2] Smith, L. G., "A Theoretical Study of the Torques Induced by a Magnetic Field on Rotating Cylinders and Spinning Thin-Wall Cones, Cone Frustums, and General Body of Revolution," TR-R-129, 1962, NASA.

[3] Petrovsky, I. G., *Lectures on Partial Differential Equations*, Interscience Publishers, New York, 1954, pp. 192–196.

[4] "The Radiation Environment," Fourth Weather Group, 4WGP-80-6-1, June 1, 1965, Andrews Air Force Base, Washington, D. C.

[5] Dandanell, E. A., "Solar Torque Model," internal memo, to D. D. James, Honeywell, Inc., Minneapolis, Minn., March 1, 1968.

[6] Beletskii, V. V., "Motion of an Artificial Satellite About Its Center of Mass," TT F-429, 1966, NASA.

[7] Nelson, G. D. and Arneson, G. R., "The Development and Performance of an Attitude Determination Data Reduction and Analysis System," Aerospace Corporation Attitude Determination Symposium, Sept. 30, Oct. 1–2, 1969, El Segundo, Calif.

[8] Foudriat, E. C., "The Limit Memory Attitude Determination System using Simplified Equation of Motion," paper presented at Aerospace Corporation Attitude Determination Symposium, Sept. 30, Oct. 1–2, 1969.